ANALYSIS OF TRACKING DATA USING NORMAL FORMS

F. Neri and A.J. Dragt
Department of Physics and Astronomy
University of Maryland
College Park, Maryland 20742

Introduction

We assume that the reader has some understanding of Lie algebraic methods as applied to classical dynamics (for an introduction, see (1) and references therein). One of the capabilities of a Lie algebraic code, like MARYLIE, is to generate a "map", the nonlinear analog of a transport matrix, and the ability to compose such maps. If we write the map that transports a particle around a circular machine as M, then it can be shown that (up to divergences), there is a map A such that

$$M = A^{-1} N A \quad (1)$$

Here N is the normal form of the map. Assuming that the map M is static (no bunchers or accelerating cavities), then N can be written as

$$N = \exp(-:H:) \quad (2)$$

Here H (the pseudo Hamiltonian) is a polynomial, which has only a few nonzero terms. Up to third order, in the static case H can be written as (if the tunes have no second, third or fourth order resonance):

$$\begin{aligned} H = &(w_x + w_x' p_\tau + \frac{w_x''}{2} p_\tau^2)\, h_x \\ &+ (w_y + w_y' p_\tau + \frac{w_y''}{2} p_\tau^2)\, h_y \\ &+ a h_x^2 + b h_x h_y + c h_y^2 + d p_\tau^2 + e p_\tau^3 + f p_\tau^4 \\ &+ \text{higher order terms.} \end{aligned} \quad (3)$$

Here $h_x = \frac{x^2 + p_x^2}{2}$, $h_y = \frac{y^2 + p_y^2}{2}$.

Note that eq. 3 has only 12 independent parameters, while a generic fourth order polynomial in six variables has 209 coefficients. The coefficients of H have an immediate physical meaning: $\frac{w_x}{2\pi}$, $\frac{w_y}{2\pi}$ are the tunes, $\frac{w_x'}{2\pi}$, $\frac{w_y'}{2\pi}$ are the first order chromaticities, $\frac{a}{2\pi}$ is the horizontal anharmonicity, the unit change of the tune for an unit charge in emittance. We see that N describes the ideal, uncoupled betatron motion. A describes the distortion of the ideal motion. Note that N is the same at any point of the ring, while A is dependent on the point of section. Eq. (1) can be interpreted in the following way: A^{-1} changes from the actual phase space variables to the normal variables, then N applies the normal Hamiltonian to the normal variables, finally A changes back to the actual phase space. This is equivalent to applying the one-turn map to the actual coordinates. The motion in the normal variables is very simple. If one goes to action angle coordinates defined by

$$\xi_x = x + ip_x = \sqrt{2h_x}\, e^{-i\phi_x}$$

$$\xi_y = y + ip_x = \sqrt{2h_y}\, e^{-i\phi_x}. \quad (4)$$

One can see that the action of H does not change h_x and h_y, while ϕ_x, ϕ_y change by a phase shift dependent only on h_x, h_y.

Thus the motion in the normal form coordinates lies on the direct product of a circle in the x-p_x plane and a circle in the y-p_y plane.

Data Analysis in the Nonresonant Case

The producedure for analyzing the tracking data is as follows.

(1) A map is produced for the whole ring using a program that can do it (not necessarily MARYLIE).

(2) MARYLIE is used to analyze the map, giving the map A^{-1}. The current version of MARYLIE can do this to third order. An advanced version of MARYLIE produce A^{-1} up to fifth order (see also reference 2).

(3) One then applies A^{-1} to the tracking data, which itself can be produced using any program.

If the resulting "cleaned up" data lies on perfect circles one can deduce that any "smear" present in the initial tracking data is not the product of the motion being chaotic, but can in fact be closely approximated by an integrable system.

Any residual smear is a candidate for real chaos. The normal form procedure thus acts as a microscope to reveal a small region of chaos in the tracking data. Of course residual smear can also be caused by the truncations used when producing M and computing the factorization of eq. 1.

As an example, figure 1 shows tracking data for the Tevatron with strong distortion sextupoles turned on. Both horizontal and vertical oscillations are excited. The large areas of "random" motion could be interpreted as chaos. By contrast the data in figure 2 has been transformed by A^{-1}. The data lies very close to circles, showing that the original data lies close to distorted four dimensional tori, ,and most of the apparent smear is due to the projection into two dimensions of the distorted tori. Since h_x, h_y are invariant for the normal motion, by applying A^{-1} to them one can derive approximate invariants under the actual motion. Such invariant are the nonlinear analogs of the linear Courant-Snyder invariants. Figure 3 compares these invariants, computed to fourth and sixth order with the Courant-Snyder invariants.

Resonant Case

If the tunes are resonant a normal form like the one in eq. 3 is not possible. Assume we have $w_x = w_y$, then we can still write

$$M = A^{-1} N_{Res} A\,,$$

with

$$\mathcal{N}_{Res} = \exp(-:H_{Res}:)$$

H_{Res} has (up to fourth order) the following additional terms besides the ones in eq. 3:

$$\begin{aligned} H_{Res} = H &+ \alpha \operatorname{Re} \xi_x \bar{\xi}_y p_\tau + \beta \operatorname{Im} \xi_x \bar{\xi}_y p_\tau \\ &+ \gamma \operatorname{Re} \xi_x \bar{\xi}_y p_\tau^2 + \delta \operatorname{Im} \xi_x \bar{\xi}_y p_\tau^2 \\ &+ A \operatorname{Re} \xi_x^2 \bar{\xi}_y^2 + B \operatorname{Im} \xi_x^2 \bar{\xi}_y^2 \\ &+ C \operatorname{Re} \xi_x \bar{\xi}_y h_x + D \operatorname{Im} \xi_x \bar{\xi}_y h_y \\ &+ E \operatorname{Re} \xi_y \bar{\xi}_y h_y + F \operatorname{Im} \xi_x \bar{\xi}_y h_x. \end{aligned} \tag{5}$$

The terms in eq. 4 commute with the quadratic part of the Hamiltonian

$$w\left(\frac{h_x}{2} + \frac{h_y}{2}\right) + d\,\frac{p_\tau^2}{2}.$$

As a function of action-angle variables the resonant terms can be written as

$$\begin{aligned} &2 h_x^{1/2} h_y^{1/2} (\alpha \cos(\phi_y - \phi_x) + \beta \sin(\phi_y - \phi_x))\, p_\tau \\ &+ 2 h_x^{1/2} h_y^{1/2} (\gamma \cos(\phi_y - \phi_x) + \delta \sin(\phi_y - \phi_x))\, p_\tau^2 \\ &+ 4 h_x h_y (A \cos(2\phi_y - 2\phi_x) + B \sin(2\phi_y - 2\phi_x)) \\ &+ 2 h_x^{3/2} h_y^{1/2} (C \cos(\phi_y - \phi_x) + D \sin(\phi_y - \phi_x)) \\ &+ 2 h_x^{1/2} h_y^{3/2} (E \cos(\phi_y - \phi_x) + D \sin(\phi_y - \phi_x)). \end{aligned} \tag{6}$$

Since the extra terms in the effective Hamiltonian only dependent on $\phi_y - \phi_x$, they commute with $h_x + h_y$. This has been shown here to fourth order, but it can easily be seen to be true to arbitrary order. This suggests to go to a new canonical set of coordinates. Instead of ϕ_x, h_x, ϕ_y, h_y one can use

$$\begin{aligned} \phi_1 &= \phi_x \qquad & h_1 &= h_x + h_y \\ \phi_2 &= \phi_y - \phi_y \qquad & h_2 &= h_y. \end{aligned} \tag{7}$$

The variables ϕ_i, h_i are canonically conjugate:

$$[\phi_i, h_j] = \delta_{ij}. \tag{8}$$

In these new coordinates H_{Res} commutes with h_1 and is only a function of ϕ_2, h_1 and h_2. Since h_1 is constant, in the ϕ_2, h_2 plane, the trajectories lie on the contour lines of H_{Res}, for a given value of h_1.

One can introduce cartesian coordinates using the identities

$$\begin{aligned} (q_1 + ip_1) &= \sqrt{2h_1}\, e^{-i\phi_1} \\ (q_2 + ip_2) &= \sqrt{2h_2}\, e^{-i\phi_2}. \end{aligned} \tag{9}$$

In these new variables the motion is on a torus given by the direct product of a circle in the q_1, p_1 plane and a closed curve in the q_2, p_2 plane. Note that the speed of motion around the circle in the q_1-p_1 plane is not constant, since the rate of change of ϕ_1 is a function of h_2 and ϕ_2.

The change from x, p_x, y, p_y to q_1, p_1, q_2, p_2 can be written directly in the cartesian form:

$$\begin{aligned} q_1 &= \frac{x}{\sqrt{x^2 + p_x^2}} \sqrt{x^2 + p_x^2 + y^2 + p_y^2} \\ p_1 &= \frac{p_x}{\sqrt{x^2 + p_x^2}} \sqrt{x^2 + p_x^2 + y^2 + p_y^2} \\ q_2 &= \frac{xy + p_x p_y}{\sqrt{x^2 + p_x^2}} \\ p_2 &= \frac{x p_y - y p_x}{\sqrt{x^2 + p_x^2}}. \end{aligned} \tag{10}$$

The cartesian form shows that the coordinates q_2, p_2 are singular at the point corresponding to $x = p_x = 0$, which is a fixed point for H_{Res}.

In the q_2, p_2 plane this fixed point is mapped into a circle of radius $\sqrt{2h_1}$. Only the region inside the circle is accessible to physical motion. This suggests to "regularize" the coordinates by mapping the inside of the circle into the surface of a sphere with the center mapped into the south pole and the circumference into the north pole. The radii are mapped to meridians. The area is preserved by considering the q_2-p_2 plane picture as a Lambert-equiarea projection. The radius of the sphere is $R = \sqrt{\frac{h_1}{2}}$. The procedure for the resonant case add to the steps of the nonresonant case the final transformation given in eq. 10. As a simple example fig. 4 shows the results of tracking a superperiod of the LHC lattice (the SUPPER lattice of ref. 3).

Figure 5 shows the same data after the application of the resonant A^{-1}, followed by the transformation of eq. 10. Figure 6 shows the same data plotted on a sphere.

References

1. A.J. Dragt et al., Lie Algebraic Treatment of Linear and Nonlinear Beam Dynamics, to appear in Ann. Rev. Nuclear and Particle Science, vol. 38 (1988); A.J. Dragt, Lie Algebraic Methods, Nuc. Inst. and Methods A258 (1987) 339-356 and references therein. See also the MARYLIE manual.

2. E. Forest, M. Berz and J. Irwin, Normal Form Methods etc., SSC Report SSC-166 (1988).

3. L.M. Healy, Anharmonicity Studies with MARYLIE and MAD, LEP Note 585 (1987). See also E. Keil, Tune Shift with Amplitude in the LHC, LEP Division report to be published.

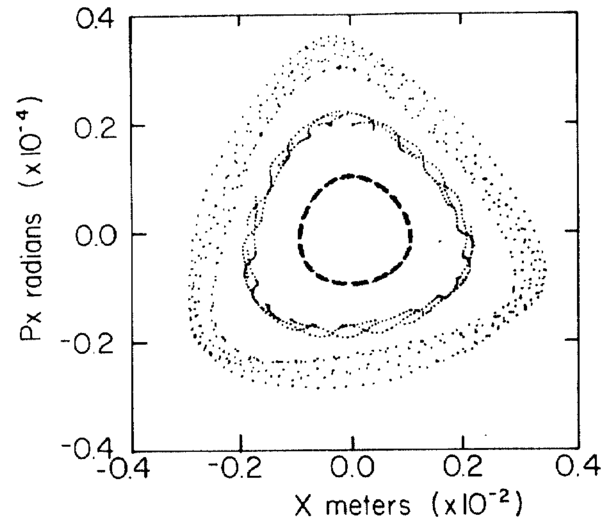

Fig. 1. Tracking data for the TEVATRON with distortion sextupoles. Both horizontal and vertical motion is excited.

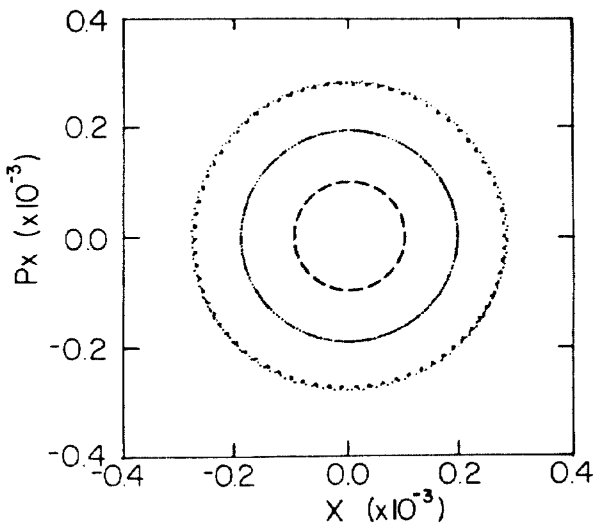

Fig. 2. The data of fig. 1 transformed by the non-resonant A^{-1}. Units are (m x radians)$^{1/2}$.

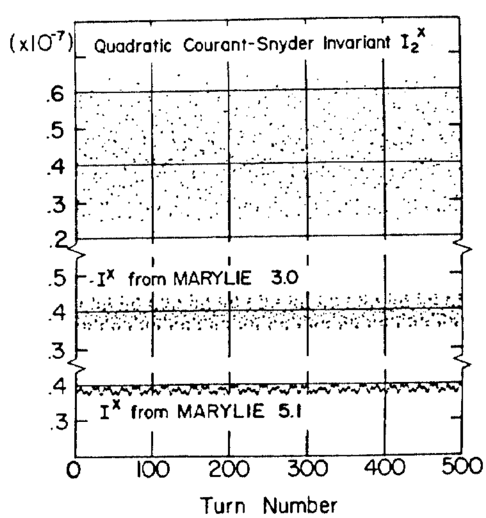

Fig. 3. Nonlinear invariants for the outer trajectory of fig. 1.

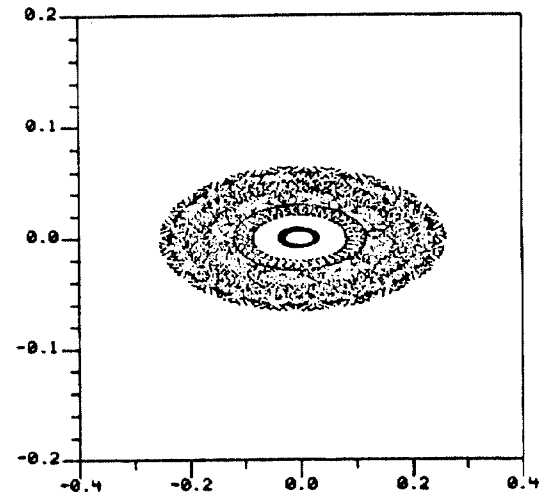

Fig. 4. Tracking data for the LHC. Six orbits are shown. The tunes are very close $\nu_x = \nu_y = 16.57$.

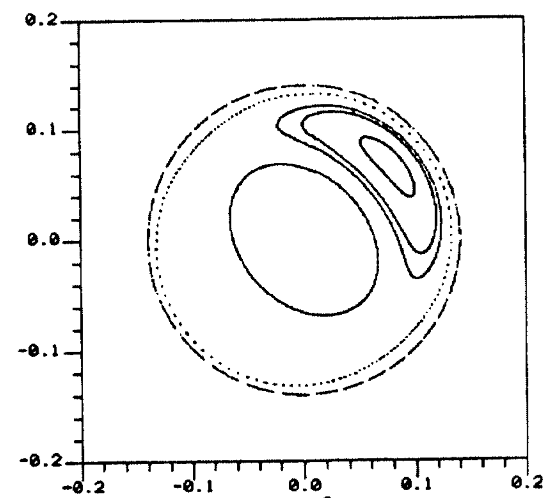

Fig. 5. The orbits of fig. 4. transformed by the resonant A^{-1}. The variables q_2 and p_2 of eq. 10 are shown. Units are (m x radians)$^{1/2}$ x 10^{-2}.

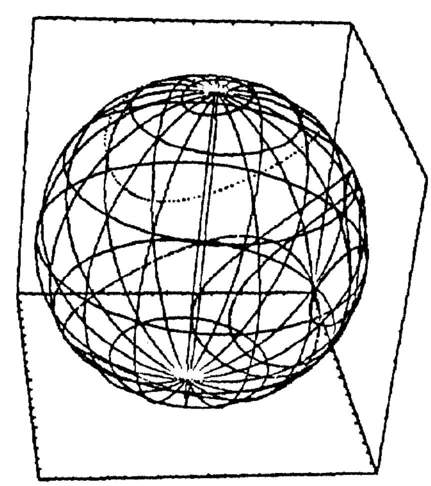

Fig. 6. The same data as in fig. 5 plotted on a sphere.